

Artifact Rates for 2D Retinal Nerve Fiber Layer Thickness Versus 3D Retinal Nerve Fiber Layer Volume

Stephanie Choi¹, Firas Jassim², Edem Tsikata², Ziad Khoueir^{2,3}, Linda Y. Poon^{2,4}, Boy Braaf⁵, Benjamin J. Vakoc⁵, Brett E. Bouma^{5,6,7}, Johannes F. de Boer^{8,9}, and Teresa C. Chen²

¹ Harvard Medical School, Department of Ophthalmology, Boston, MA, USA

² Harvard Medical School, Department of Ophthalmology, Massachusetts Eye and Ear Infirmary, Glaucoma Service, Boston, MA, USA

³ Beirut Eye and ENT Specialist Hospital, Saint-Joseph University Medical School, Beirut, Lebanon

⁴ Department of Ophthalmology, Kaohsiung Chang Gung Memorial Hospital, Chang Gung University College of Medicine, Kaohsiung, Taiwan

⁵ Wellman Center for Photomedicine, Massachusetts General Hospital, Boston, MA, USA

⁶ Institute for Medical Engineering and Science, Massachusetts Institute of Technology, Cambridge, MA, USA

⁷ Harvard Medical School, Division of Health Sciences and Technology, Cambridge, MA, USA

⁸ LaserLaB Amsterdam, Department of Physics and Astronomy, Vrije Universiteit, Amsterdam, The Netherlands

⁹ Department of Ophthalmology, Amsterdam UMC, Amsterdam, The Netherlands

Correspondence: Teresa C. Chen, Harvard Medical School, Department of Ophthalmology, Massachusetts Eye and Ear Infirmary, Glaucoma Service, 243 Charles St, Boston, MA 02114, USA. e-mail: teresa_chen@meei.harvard.edu

Received: August 18, 2019

Accepted: November 24, 2019

Published: February 12, 2020

Keywords: optical coherence tomography; glaucoma; RNFL artifacts

Citation: Choi S, Jassim F, Tsikata E, Khoueir Z, Poon LY, Braaf B, Vakoc BJ, Bouma BE, de Boer JF, Chen TC. Artifact rates for 2D retinal nerve fiber layer thickness versus 3D retinal nerve fiber layer volume. *Trans Vis Sci Tech.* 2020;9(3):12, <https://doi.org/10.1167/tvst.9.3.12>

Purpose: To compare artifact rates in two-dimensional (2D) versus three-dimensional (3D) retinal nerve fiber layer (RNFL) scans using Spectralis optical coherence tomography (OCT)

Methods: Thirteen artifact types in 2D and 3D RNFL scans were identified in 106 glaucomatous eyes and 95 normal eyes. Artifact rates were calculated per B-scan and per eye. In 3D volume scans, artifacts were counted only for the 97 B-scans used to calculate RNFL parameters for the 2.5–3.5-mm annulus. 3D RNFL measurements were calculated twice, once before and again after deletion of B-scans with artifacts and subsequent automated interpolation.

Results: For 2D scans, artifacts were present in 58.5% of B-scans (62 of 106) in glaucomatous eyes. For 3D scans, a mean of 35.4% of B-scans (34.3 of 97 B-scans per volume scan) contained an artifact in 106 glaucomatous eyes. For 3D data of glaucoma patients, mean global RNFL thickness values were similar before and after interpolation ($77.0 \pm 11.6 \mu\text{m}$ vs. $75.1 \pm 11.2 \mu\text{m}$, respectively; $P = 0.23$). Fewer clinically significant artifacts were noted in 3D RNFL scans, where only 7.5% of glaucomatous eyes (8 of 106) and 0% of normal eyes (0 of 95) had artifacts, compared to 2D RNFL scans, where 58.5% of glaucomatous eyes (62 of 106) and 14.7% of normal eyes (14 of 95) had artifacts.

Conclusions: Compared to 2D RNFL scans, 3D RNFL volume scans less often require manual correction to obtain accurate measurements.

Translational Relevance: 3D RNFL volume scans have fewer clinically significant artifacts compared to 2D RNFL thickness scans.

Introduction

Retinal nerve fiber layer (RNFL) thinning is a hallmark of glaucoma, the leading cause of irreversible blindness worldwide.^{1–3} Because such structural changes often precede visual field defects,

optical coherence tomography (OCT) RNFL thickness measurements can assist in diagnosing and monitoring disease progression.^{2–4} Unlike traditional time-domain optical coherence tomography, spectral-domain optical coherence tomography (SD-OCT) allows for three-dimensional (3D) datasets and has higher resolution and faster acquisition speeds.^{5,6}

Recent literature has suggested that RNFL volume measurements from 3D datasets may be the same or better than two-dimensional (2D) RNFL thickness measurements for diagnosing glaucoma.⁷⁻⁹

Although 2D RNFL thickness is currently the most commonly used OCT parameter for evaluating glaucoma, its usefulness is limited by high artifact rates. In a retrospective study of 277 consecutive patients with glaucoma, the authors found that 19.9% of RNFL scans contained at least one artifact.¹⁰ In another retrospective study of 2313 eyes, the authors found that 46.3% of RNFL scans had at least one artifact, and an increased prevalence of artifacts was associated with worse visual acuity, more severe cataracts, and advanced glaucoma.¹¹

Our study sought to determine if 3D RNFL volume measurements are associated with fewer artifacts. We therefore compared the frequency of artifacts in 3D volume scans versus 2D RNFL scans in both normal and glaucoma patients. A secondary goal was to determine if correction of artifacts through interpolation of 3D datasets was clinically necessary.

Methods

Study Population

Adult subjects who underwent a complete ophthalmic examination in the Glaucoma Service at the Massachusetts Eye and Ear (MEE) by T.C.C. were recruited between April 2009 and January 2016. The study was approved by the MEE Review Board and conducted in accordance with the tenets of the Declaration of Helsinki. All eligible participants consented to Spectralis SD-OCT (Spectralis software version 5.4.8.0; Heidelberg Engineering, Heidelberg, Germany) scanning on the same day as their examination, which included history, visual acuity, refraction, Goldman applanation tonometry, slit-lamp biomicroscopy, gonioscopy, dilated ophthalmoscopy, ultrasound pachymetry (PachPen[®]; Accutome, Inc., Malvern, PA), stereo disc photography (Visucam[®]PRONM; Carl Zeiss Meditec, Inc., Dublin, CA), and Humphrey visual field testing (Swedish Interactive Threshold Algorithm 24-2 test; Carl Zeiss Meditec, Inc.).

Subjects were included if they had a spherical equivalent between -5 and $+5$ diopters, best-corrected visual acuity of 20/40 or better, and reliable visual field testing defined as $\leq 33\%$ fixation losses, $\leq 20\%$ false-positives, and $\leq 20\%$ false-positives. Glaucoma staging was modeled after the Hodapp-Anderson-Parrish criteria: (1) early glaucoma (-6 dB \leq mean

deviation [MD] ≤ 0 dB), (2) moderate glaucoma (-12 dB \leq MD < -6 dB), and (3) advanced glaucoma (MD < -12 dB).

Subjects were excluded if they had anterior segment dysgenesis, corneal scarring, corneal opacities, non-glaucomatous field loss (e.g., diabetic retinopathy), or dilated pupil diameter less than 2 mm. For subjects whose eyes were both eligible for the study, one eye was selected randomly for analysis.

Normal subjects consisted of those without ocular disease except for mild cataracts, and glaucoma patients had characteristic optic nerve changes with corresponding abnormal visual field defects. Only perimetric open-angle glaucoma patients were included. Visual fields were abnormal if three or more contiguous locations in the pattern standard deviation plot were depressed at the $P < 0.05$ level or if at least two contiguous locations were depressed at the $P < 0.05$ level and one at the $P < 0.01$ level.

Optical Coherence Tomography Imaging

All SD-OCT imaging was performed after pupillary dilation. Imaging was performed using Spectralis SD-OCT version 5.4.8.0, which has an acquisition rate of 40,000 A-lines per second. Criteria for determining adequate scan quality included 2D OCT signal strength greater or equal to 15 (range, 0–40 dB).

For 2D scans, the commercially available Spectralis SD-OCT version 5.4.8.0 was used, and RNFL thickness was calculated along a 12° peripapillary scan circle around the optic nerve, approximately 3.5 to 3.6 mm depending on the axial eye length, with the averaging function turned on. Patients with OCT signal strength of less than 15 were excluded from the analysis. The Spectralis SD-OCT software automatically segmented the anterior and posterior RNFL to calculate the average RNFL thickness for the overall globe (360°), for each quadrant (i.e., superior, temporal, inferior, and nasal, each 90°), and for designated octants (i.e., superior-temporal, superior-nasal, inferior-nasal, and inferior-temporal, each 45°). Artifacts were identified based on the raw image for the RNFL, as some artifacts were not evident based only on color classifications.¹⁰

From 3D volumetric scans, RNFL volume and thickness parameters were calculated using custom-designed software from our research group. Volume scans contained 193 B-scans centered on the optic nerve head and over a $20 \times 20^\circ$ field (or approximately 6×6 -mm area). Three frames were averaged at each position. Each volume scan was then processed using a segmentation algorithm that is not commercially available and was developed by our research group with MATLAB 2012a (MathWorks, Inc., Natick, MA).

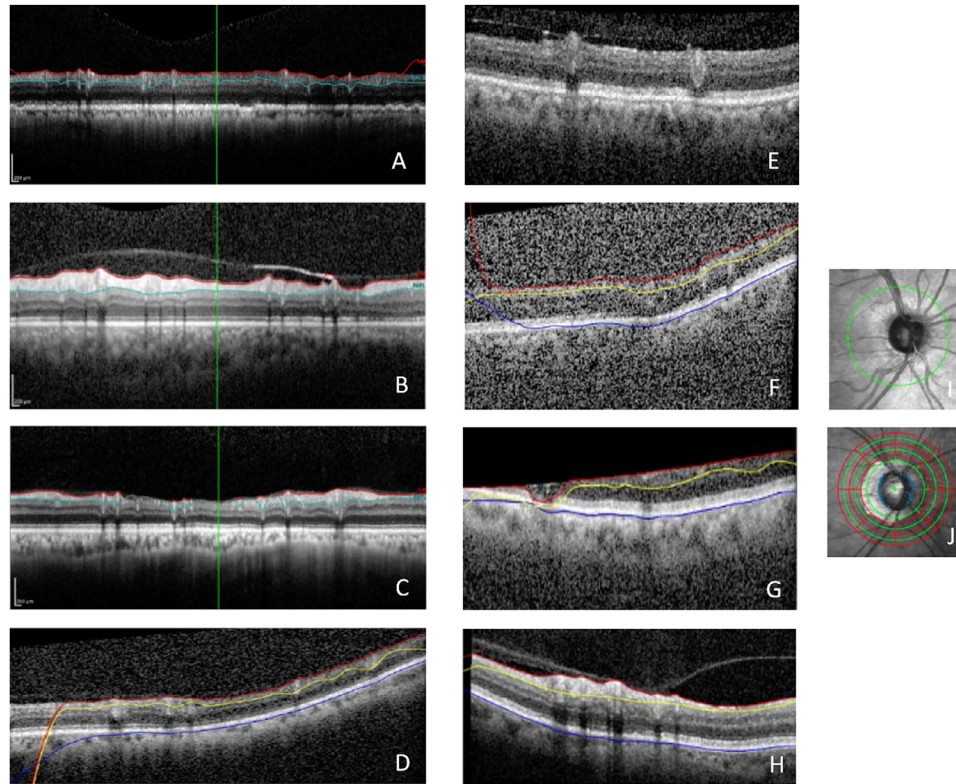


Figure 1. Examples of artifact types found in 2D and 3D images. (A) Incorrect segmentation of the anterior RNFL (red line). (B) Misidentification of the anterior RNFL due to a posterior vitreous detachment (red line). (C) Incorrect segmentation of the posterior RNFL (blue line). (D) Incorrect segmentation of the internal limiting membrane (red line), posterior RNFL (yellow line), and RPE (dark blue line). (E) Complete segmentation failure, despite clearly identifiable anatomic layers. (F) Degraded image quality where the signal is indistinguishable from the background noise. (G) Out of register artifact resulting in truncation of retinal layers. (H) Cut edge on left-hand side of the B-scan. (I) Decentration error was defined as when the optic nerve head was greater than 10% off center. (J) Area of PPA crosses the outer border of the smallest annulus (2.5–3.5 mm).

Whereas the native Spectralis OCT software uses 2D scans to compute thickness measurements, our custom-designed software uses 3D scans to compute thickness and volume measurements.

The custom-built software identifies the center of the optic disc using the spatial information provided by the terminations of the RPE/Bruch's membrane (BM) complex and then determines peripapillary RNFL volume within four different sizes of annuli centered on the optic nerve head. Each peripapillary 3D annulus has a width of 1 mm. The smallest circumpapillary annulus 1 (CA1) is defined by an inner diameter of 2.5 mm and an outer diameter of 3.5 mm, the larger CA2 by diameters of 3 mm and 4 mm and CA3 by diameters of 3.5 mm and 4.5 mm, and the largest CA4 by diameters of 4 mm and 5 mm.⁷

For each of the 193 B-scans in the 3D volume set, automatic segmentation using edge and intensity information delineated the anterior internal limiting membrane border and the posterior retinal nerve fiber layer border, and the software calculated the average RNFL thickness and RNFL volume based on

the tissue between these two borders. Average RNFL volume and thickness was calculated using an annulus size of 2.5 to 3.5 mm, as this size has been shown to have the greatest diagnostic capability.⁷ Only the 97 B-scans lying within the annulus were analyzed for artifacts among the total 193 B-scans per volume scan.

Evaluation of Artifacts

Thirteen types of OCT artifacts were recorded for 2D and 3D RNFL scans: (1) anterior RNFL misidentification, (2) posterior vitreous detachment (PVD)/epiretinal membrane (ERM)-associated error, (3) posterior RNFL misidentification, (4) retinal pigment epithelium (RPE) misidentification, (5) complete segmentation failure, (6) degraded image, (7) out of register, (8) cut edge, (9) technician-related decentration, (10) peripapillary atrophy (PPA)-associated error, (11) motion artifact, (12) mirror/inverted scan, and (13) missing parts. RPE misidentification applied only to 3D datasets (Fig. 1D),

because the 3D algorithm automatically segmented the RPE before the posterior RNFL border.

Anterior RNFL, posterior RNFL, and RPE misidentification occurred with incorrect segmentation (Figs. 1A–1D). Artifacts associated with PVDs and ERMs were counted only if they led to artifactually thick or thin RNFL values and were categorized as a subset of anterior RNFL misidentification artifacts (Fig. 1B). Complete segmentation failures occurred with the total absence of segmentation by the algorithm (Fig. 1E).

Degraded images occurred when the parts of the image signal were indistinguishable from the background noise, and these images were often associated with segmentation errors (Fig. 1F). Out of register artifacts occurred when there was truncation of some of the retinal layers due to superior or inferior shift of the scan (Fig. 1G).

Cut edge artifacts were defined as scans with abrupt lateral edge truncation of the RNFL scan (Fig. 1H). Technician-related decentration artifacts appeared when the center of the optic nerve head was more than 10% off the center of the peripapillary scan (Fig. 1I). PPA-associated artifacts occurred when the region of PPA crossed over the 12° peripapillary scan circle (Fig. 1J). For 3D RNFL scans, PPA-associated artifacts were counted only if the area of PPA crossed the smallest annulus (2.5–3.5 mm), the primary annulus size used for this study.

Motion artifacts were recorded when patient movement was significant enough to cause the RNFL to be out of the rectangular display on the printout. Mirrored or inverted scans consisted of scans with flipping of the retinal image due to images crossing the zero-time delay line. Finally, missing parts occurred when a portion of the RNFL scan was missing due to either a blink or vitreous opacity.

Interpolation and Correction of Artifacts

Custom-designed MATLAB software calculated 3D RNFL volume and thickness parameters. These parameters were calculated with and without correction for artifacts. For the former, frames with artifacts were manually deleted, and the software then recalculated RNFL volume and thickness parameters after interpolation of deleted frames. For 3D volume scans, clinically significant artifacts were those determined to cause pre- and post-interpolation values to be statistically different and therefore would require manual correction in the clinic. For 2D RNFL scans, manual correction of segmentation errors was not conducted in this study because a clinically significant

artifact was one that would require manual correction in the clinic.

Statistical Analysis

All statistical analyses were performed using Stata[®] 15 (StataCorp, College Station, TX). Demographic and ocular characteristics were compared with χ^2 tests for categorical variables and two-tailed Student's *t*-tests for continuous variables. To quantify the frequency of artifacts for 2D scans, the number of B-scans with at least one artifact was divided by the total number of eyes, as each eye had only one B-scan. For 3D scans, both the proportion of volume scans with any artifacts and the proportion of B-scans with artifacts per eye were determined. To calculate the latter (i.e., artifact rate per eye), the number of B-scans with at least one artifact was divided by 97, the total number of B-scans within the smallest-sized annulus. Scans with multiple artifacts were only counted once. Results were statistically significant if $P < 0.05$.

Results

Patient Characteristics

Table 1 shows that the characteristics of the glaucoma versus normal groups were similar, except that the glaucoma group was significantly older (67.6 ± 12.1 years vs. 53.6 ± 16.7 years; $P < 0.001$) and had worse mean deviation compared to the normal group (-12.5 ± 7.9 vs. -1.7 ± 2.3 ; $P < 0.001$).

Frequency of 2D Artifacts for Normal Versus Glaucoma Patients

For 2D RNFL circular scans, OCT artifacts were more common in glaucoma compared to normal subjects (58.5% vs. 14.7%; $P < 0.001$) (Table 2), with posterior RNFL misidentification error being the most common artifact in glaucoma patients (46.2% for glaucoma vs. 5.3% for normal subjects; $P < 0.001$) (Table 2). Several 2D RNFL artifacts reported in the literature were not observed in our study population, including complete absence of segmentation, out of register, cut edge, mirroring, missing parts, and motion artifacts (Table 2).¹¹

Frequency of 3D Artifacts for Normal Versus Glaucoma Patients

Although each 3D 6×6 -mm volume scan contained a total of 193 B-scans, artifact rates were determined

Table 1. Demographic Characteristics of the Normal and Glaucoma Study Populations

Characteristic	Glaucoma	Normal	<i>P</i>
Total number of eyes	106	95	—
Right eyes/left eyes (<i>n</i>)	58/48	57/38	0.45
Male/female (<i>n</i>)	51/55	37/58	0.19
Age (y), mean ± SD (range)	67.6 ± 12.1 (21–87)	53.6 ± 16.7 (18–87)	<0.001 ^{***}
Refractive error			
Spherical equivalent (diopters), mean ± SD	−0.6 ± 1.8	−0.4 ± 1.7	0.45
Visual field			
Mean deviation (dB), mean ± SD	−12.5 ± 7.9	−1.7 ± 2.3	<0.001 ^{***}
Pattern standard deviation (dB), mean ± SD	8.4 ± 3.4	1.7 ± 0.5	<0.001 ^{***}

^{***}Results are statistically significant.

Table 2. Percentage of 2D Retinal Nerve Fiber Layer Scans with Artifacts

Artifact Type	Glaucoma (<i>n</i> = 106) Percentage of B-scans (%) ^a	Normal (<i>n</i> = 95) Percentage of B-scans (%) ^a	<i>P</i>
Posterior RNFL misidentification	46.2	5.3	<0.001 ^{***}
Decentration	10.4	8.4	0.64
Anterior RNFL misidentification	9.4	3.2	0.07
PVD/ERM	4.7	2.1	0.32
Degraded image	2.8	0	0.10
Peripapillary atrophy	1.9	0	0.18
Complete absence of segmentation	0	0	N/A
Out of register	0	0	N/A
Cut edge	0	0	N/A
Mirroring	0	0	N/A
Missing parts	0	0	N/A
Motion artifact	0	0	N/A
Any artifact (total percentage) ^b	58.5	14.7	<0.001 ^{***}

^aProportion of 2D retinal nerve fiber layer scans with the specified artifact type divided by 106 for the glaucoma group and 95 for the normal group.

^bTotal percentage represents the total percentage of 2D retinal nerve fiber layer scans with at least one artifact type. Scans with multiple artifacts were only counted once.

^{***}Results are statistically significant.

only for the 97 B-scans comprising the smallest annulus (2.5–3.5 mm), the annulus size suggested to have the greatest diagnostic ability.⁷ For both normal and glaucoma subjects, in all of the volume scans at least one of the 97 B-scan frames contained an artifact. Compared to volume scans of normal eyes, the volume scans of glaucomatous eyes had a higher percentage of B-scans with artifacts (mean of 35.4% of the 97 B-scans vs. 21.8% of the 97 B-scans; *P* < 0.001) (Table 3). Glaucoma patients had a significantly higher rate of posterior RNFL segmentation artifacts compared to the normal group with a mean of 21.9% of 97 B-scans versus 15.5% of 97 B-scans (*P* = 0.002) (Table 3).

Frequency of 2D Versus 3D Artifacts for Glaucoma Patients

Among the 106 glaucoma patients, 3D OCT scans contained fewer artifacts per B-scan compared to 2D OCT scans (35.4% of 97 B-scans vs. 58.5% of B-scans; *P* < 0.001) (Tables 2 and 3).

3D RNFL Calculations With and Without Correction for Artifacts

Table 4 demonstrates mean global RNFL thickness values derived from 3D volume scans before and after interpolation. For 8 of the 106 glaucoma

Table 3. Percentage of B-Scans with Artifacts in 3D Volume Scans (Smallest Annulus Size of 2.5–3.5 mm)

Artifact Type	Glaucoma (%) (n = 106) ^a	Normal (%) (n = 95) ^a	P
Posterior RNFL misidentification	21.9	15.5	0.002***
RPE misidentification	5.8	4.9	0.38
Anterior RNFL misidentification	3.8	2.4	0.23
PVD/ERM	1.9	1.2	0.33
Out of register	2.9	2.7	0.89
Peripapillary atrophy	2.0	0.4	0.10
Degraded	1.3	0.7	0.20
Cut edge	0.3	0.6	0.39
Complete absence of segmentation	0.1	0.1	0.65
Mirroring	0.1	0.2	0.77
Motion artifact	0	0	N/A
Any artifact (total percentage) ^b	35.4	21.8	<0.001***

^aPercentage of artifacts per eye was calculated as the number of B-scans with artifact type divided by 97, which was the total number of B-scans per volume scan that contributed to calculations for the smallest sized annulus (2.5–3.5 mm).

^bTotal percentage represents the total percentage of B-scans within a volume scan with at least one artifact type. Scans with multiple artifacts were only counted once.

***Results are statistically significant.

Table 4. Global Retinal Nerve Fiber Layer Thickness Derived Using 3D Volume Scans, Pre- and Post-Interpolation (Annulus Size 2.5–3.5 mm)

	Mean Global RNFL Thickness Pre-Interpolation Thickness (μm) ^a	Mean Global RNFL Thickness Post-Interpolation Thickness (μm) ^a	P	Mean Absolute Percentage Difference (Pre- vs. Post-Interpolation)	Standard Deviation of Percentage Difference (Pre- vs. Post-Interpolation)	P
Glaucoma (n = 98) ^b	77.0 ± 11.6	75.1 ± 11.2	0.23	0.03%	4.7%	0.94
Normal (n = 95)	104.0 ± 10.6	104.0 ± 10.0	0.98	0.1%	3.3%	0.68

^aResults are presented as mean ± standard deviation.

^bMATLAB software reported blank values for 8 patients after interpolation. Average global retinal nerve fiber layer thickness was recalculated using the remaining 98 of 106 glaucoma patients.

patients (7.5%), the MATLAB software was unable to fully interpolate images and was thus unable to calculate RNFL volume and thickness parameters despite manual deletion of frames with artifacts. This issue occurred if too many of the 193 B-scans could not be accurately segmented using automated techniques. Because the algorithm was unable to calculate interpolated images for these 8 patients, average global RNFL volume and thickness was calculated using the remaining 98 glaucoma patients. The mean global RNFL thickness values were statistically similar for both the glaucoma sample (77.0 ± 11.6 μm pre-interpolation vs. 75.1 ± 11.2 μm post-interpolation; $P = 0.23$) and normal sample (104.0 ± 10.6 μm pre-interpolation vs. 104.0 ± 10.0 μm post-interpolation; $P = 0.98$). In addition, interpolation did not significantly change

individual RNFL thickness values for glaucomatous eyes and normal eyes, with mean absolute percentage differences in pre- and post-interpolation values of 0.03% ($P = 0.94$) and 0.1% ($P = 0.68$), respectively.

Discussion

Our study has demonstrated that for glaucoma eyes, not only do 3D RNFL volume scans have fewer artifacts per B-scan compared to 2D peripapillary RNFL scans (34.5% of the 97 B-scans vs. 58.5% of B-scans) (Tables 2 and 3) but 3D RNFL volume scans also have fewer clinically significant artifacts compared to 2D peripapillary RNFL scans (7.5%, or

8 of 106 volume scans, compared to 58.5% of B-scans) (Tables 2 and 4). To our knowledge, no prior studies have directly compared 2D and 3D RNFL artifact rates. The presence of artifacts in 2D RNFL scans has posed a problem for clinicians as artifacts often render a scan unusable. Our findings show that even 3D RNFL volume scans with artifacts do not require manual correction with interpolation, because average RNFL thickness values from volume scans pre- and post-interpolation are statistically similar. Moreover, only a small percentage of volume scans (7.5%, or 8 of 106 glaucoma eyes) have clinically significant artifacts where 3D RNFL data cannot be corrected for with interpolation.

Very few artifact studies have used 3D scans of the optic nerve head region, and past studies have used different definitions of artifact rates for 3D volume data. For example, 3D artifact rates have been reported on a per volume scan basis (e.g., 42.2%, or 27 of 42 volume scans with at least one artifact).¹² When the current study used this method, we found 100% of volume scans had at least one B-scan with an artifact. Past studies have also calculated artifact rates on a per B-scan basis with the denominator being the total number of B-scans for the entire composite study population (e.g., 21.2%, or 6360 of 30,060 B-scans [167 B-scans \times 180 patients] with at least one artifact).¹² In contrast, our study calculated artifact rates per B-scan for each eye. Specifically, when analyzing 3D artifact rates in volume scans, only the 97 B-scans of the smallest annulus (2.5–3.5 mm) were analyzed, as this annulus size has been suggested to have the highest diagnostic potential.⁷ In the current study, glaucomatous eyes compared to normal eyes had a higher percentage of B-scans with artifacts per volume scan (i.e., 35.4% of the 97 B-scans vs. 21.8% of the 97 B-scans; $P < 0.001$) (Table 3). It is difficult to directly compare the current study with past studies due to differing definitions of artifact rate, SD-OCT imaging instruments, and artifact classifications. Future work on artifact rates should use clear definitions and consistent statistical methods to better allow for meaningful comparisons.

Compared to 3D volume scans, 2D RNFL scans may be more susceptible to artifacts because they are derived from one B-scan instead of a large sampling density of B-scans. The artifact rate of 2D RNFL scans among glaucomatous eyes was 58.5% (Table 2), which is higher than the range of 19.9% to 46.3% that has previously been reported in the literature.^{11,13,14} The greater frequency of 2D artifacts in our study may be attributed to the greater proportion of moderate- to advanced-stage glaucoma patients (70.8%, or 75 of 106 patients), as later stages of glaucoma have been

shown to be correlated with more artifacts.¹¹ Moreover, glaucoma suspect eyes have been associated with fewer artifacts and were excluded from our glaucoma study population.^{11–15}

Decentration can also help to explain why 2D scans may have a higher artifact rate compared to 3D scans, because 3D scans do not require manual centration of the optic nerve head. In 3D scans, the center of the optic disc is automatically identified as the RPE/BM complex border.⁷ In contrast, 2D RNFL scans require manual centration of the Spectralis circle scan around the optic nerve. In our study, the 2D decentration artifact rates were 10.4% and 8.4% for glaucoma and normal subjects, respectively (Table 2), much less than the 27.8% decentration artifact rate reported by Liu et al.¹¹ for a combined sample of glaucoma and normal subjects. As technicians become more experienced in detecting decentration errors during image acquisition, the frequency of decentration artifacts may decrease over time. Decentration artifacts are clinically relevant because they can contribute to inaccurate RNFL thickness measurements or even false-positive glaucoma diagnoses, as the RNFL is thinner as one moves away from the optic nerve head. 3D volume scans may thus provide an advantage by removing this type of artifact.^{16,17}

Our study found that glaucomatous eyes have more artifacts per B-scan than normal eyes for both 2D and 3D OCT scans. For 2D scans, 58.5% of 106 glaucomatous eyes had artifacts compared to 14.7% of 95 normal eyes ($P < 0.001$) (Table 2). For 3D scans, 35.4% of B-scans per glaucomatous eye had artifacts compared to 21.8% of B-scans per normal eye ($P < 0.001$) (Table 3). Posterior RNFL misidentification was the most common artifact type for both 2D circular and 3D volume scans and the primary source of variation in artifact frequency between glaucoma and normal subjects (Tables 2 and 3). The posterior RNFL artifact rate in 2D scans has been reported to be over 29.9% for glaucoma patients and 7.7% for all patients.^{11,14} We arrived at higher 2D posterior RNFL artifact rates for glaucoma patients (46.2% of 106 glaucomatous eyes; see Table 2), probably because our sample included more moderate- to advanced-stage glaucoma patients. Reduced RNFL reflectivity with glaucoma has been shown to lead to more algorithm failures as the posterior RNFL border becomes difficult to discern from the underlying plexiform layer.^{11,19–21} The severity of glaucoma is associated with a decrease in the RNFL attenuation coefficient, so more advanced pathology increases the likelihood of posterior RNFL misidentification.²² Only one study has reported posterior RNFL misidentification artifacts in 3D volume scans.⁷ However, the reported artifact rate was calculated on a

per B-scan composite basis (15.2%, or 4556 of 30,060 B-scans [167 B-scans \times 180 patients]), making it difficult to directly compare their population artifact rates with our individual patient artifact rates.

Our study shows that 3D RNFL artifacts do not require manual correction and interpolation, because average RNFL thickness values pre- and post-interpolation are statistically similar (Table 4). To our knowledge, no one has studied whether manual correction followed by automatic interpolation is necessary to correct RNFL artifacts in 3D volume scans. Manual refinement has been used in 2D scans to correct for segmentation errors, and this method has demonstrated significant adjustments in RNFL thickness estimates.^{15,23} Manual refinement, however, requires added time and effort and is not a practical solution during clinic. In theory, manual correction with subsequent automatic interpolation might help correct artifacts, but we found that in practice interpolation does not significantly affect RNFL measurements in volume scans. Of note, a small percentage of glaucoma patients (8 of 106, or 7.5%) had 3D RNFL data that could not be corrected for with interpolation. For all 8 of these patients, more than 75% of the B-scans within each volume scan contained artifacts. One reason to explain the high incidence of artifacts among this group is that more than half of the patients (62.5%) had advanced glaucoma with mean deviation < -12 dB, and the software algorithm may have had trouble distinguishing between retinal layers for interpolation.¹¹ Ocular pathology may also contribute to the high proportion of artifacts per volume scan. Two of the patients (25%) had many B-scans with segmentation errors secondary to the presence of an ERM. Asrani et al.¹³ found that ERM was the most common artifact type in 2D RNFL scans among glaucoma patients. One of the 8 patients had a large area of PPA that extended beyond the outer 3-mm diameter of the smallest annulus, and the presence of PPA led to degraded image quality of the B-scans. Peripapillary atrophy is notably more common and of larger size in glaucoma patients compared with normal subjects.^{24,25} Of note, we excluded all subjects with corneal scarring and corneal opacities from our study, as well as those with best corrected visual acuity worse than 20/40, so none of the patients included in the study had visually significant cataracts affecting OCT image quality.

There are several potential limitations of our study. Our population included only perimetric open-angle glaucoma patients and not glaucoma suspect or ocular hypertension patients, for whom interpretation of OCT artifacts can have important implications for diagnosis and management. Studies have shown, however, that glaucoma suspect and ocular hypertension patients

have fewer artifacts.¹¹ Another limitation was that the average age of the glaucoma patients was significantly higher than that of the normal subjects. Although some have found a relationship between segmentation errors and older age,^{14,15} others have found more artifacts with younger age.¹⁸ A study by Liu et al.¹¹ which evaluated 2313 eye scans from 1188 patients found that older age was not significantly associated with an increase in artifacts.¹¹ Given such conflicting evidence, it is unclear whether the age difference in our sample contributed to the difference in artifact rates.

3D RNFL volume scans may have similar or better diagnostic ability compared to 2D RNFL data,⁷ and our findings also show that 3D RNFL volume data have fewer clinically significant artifacts (7.5%, or 8 of 106 3D volume scans for glaucoma patients) compared to 2D RNFL data (58.5%, or 62 of 106 B-scans for glaucoma patients). This study also found that manual correction and automated interpolation of 3D volume data do not significantly change RNFL measurements. Artifacts in 2D RNFL scans continue to pose a challenge for clinicians who use imaging to assist glaucoma diagnosis and management. For 2D RNFL data, an artifact often renders the scan unusable unless manual correction or re-scanning is done. In contrast, for 3D datasets, an artifact in a single B-scan or in many B-scans can be compensated for by neighboring B-scans without artifacts; therefore, fewer 3D volume scans are rendered useless or require manual correction. Further work should be done to elucidate the clinical utility of 3D RNFL volume scans.

Acknowledgments

Supported by grant number P41EB015903 from the Center for Biomedical OCT Research and Translation, awarded by the National Institute of Biomedical Imaging and Bioengineering of the National Institutes of Health (BB, BJV, and BEB). Also supported (TCC) by the National Institutes of Health award number UL1 RR 025758, Massachusetts Lions Eye Research Fund, American Glaucoma Society Mid-Career Award, Fidelity Charitable Fund, and Department of Defense Small Business Innovation Research, DHP15-016. The funding organizations had no role in the design or conduct of this research.

Disclosure: **S. Choi**, None; **F. Jassim**, None; **E. Tsikata**, None; **Z. Khoueir**, None; **L.Y. Poon**, None; **B. Braaf**, Heidelberg Engineering (E); **B.J. Vakoc**, Terumo Corporation (P) and Ninepoint Medical (P); **B.E. Bouma**, NIDEK Inc. (P), Terumo

Corporation (P), Ninepoint Medical (P), and Heidelberg Engineering (P); **J.F. de Boer**, NIDEK Inc. (P), Terumo Corporation (P), Ninepoint Medical (P), and Heidelberg Engineering (P); **T.C. Chen**, None

References

1. Quigley H, Broman AT. The number of people with glaucoma worldwide in 2010 and 2020. *Br J Ophthalmol*. 2006;90:262–267.
2. Quigley HA, Addicks EM, Green WR. Optic nerve damage in human glaucoma: III. Quantitative correlation of nerve fiber loss and visual field defect in glaucoma, ischemic neuropathy, papilledema, and toxic neuropathy. *Arch Ophthalmol*. 1982;100:135–146.
3. Jaffe GJ, Caprioli J. Optical coherence tomography to detect and manage retinal disease and glaucoma. *Am J Ophthalmol*. 2004;137:156–169.
4. Leung CKS, Cheung CYL, Weinreb RN, et al. Evaluation of retinal nerve fiber layer progression in glaucoma: a study on optical coherence tomography guided progression analysis. *Invest Ophthalmol Vis Sci*. 2010;51:217–222.
5. Wu H, De Boer JF, Chen TC. Diagnostic capability of spectral-domain optical coherence tomography for glaucoma. *Am J Ophthalmol*. 2012;153:815–826.
6. Chen TC, Cense B, Pierce MC, et al. Spectral domain optical coherence tomography ultra-high speed, ultra-high resolution ophthalmic imaging. *Arch Ophthalmol*. 2005;123:1715–1720.
7. Khoueir Z, Jassim F, Poon LYC, et al. Diagnostic capability of peripapillary three-dimensional retinal nerve fiber layer volume for glaucoma using optical coherence tomography volume scans. *Am J Ophthalmol*. 2017;182:180–193.
8. Shin JW, Uhm KB, Seong M, et al. Retinal nerve fiber layer volume measurements in healthy subjects using spectral domain optical coherence tomography. *J Glaucoma*. 2013;57:800–807.
9. Shin JW, Uhm KB, Seong M, et al. Diffuse retinal nerve fiber layer defects identification and quantification in thickness maps. *Invest Ophthalmol Vis Sci*. 2014;55:3208–3218.
10. Asrani S, Essaid L, Alder BD, et al. Artifacts in spectral-domain optical coherence tomography measurements in glaucoma. *JAMA Ophthalmol*. 2014;132:396.
11. Liu Y, Simavli H, Que CJ, et al. Patient characteristics associated with artifacts in Spectralis optical coherence tomography imaging of the retinal nerve fiber layer in glaucoma. *Am J Ophthalmol*. 2015;159:565–576.
12. Lee SY, Kwon HJ, Bae HW, et al. Frequency, type and cause of artifacts in swept-source and cirrus HD optical coherence tomography in cases of glaucoma and suspected glaucoma. *Curr Eye Res*. 2016;41:957–964.
13. Asrani S, Essaid L, Alder BD, et al. Artifacts in spectral-domain optical coherence tomography measurements in glaucoma. *JAMA Ophthalmol*. 2014;132:396–402.
14. Wi Y-J, Yoo YC. Frequency and causes of segmentation errors in spectral domain optical coherence tomography imaging in glaucoma. *J Korean Ophthalmol Soc*. 2016;57:1407–1414.
15. Mansberger SL, Menda SA, Fortune BA, et al. Automated segmentation errors when using optical coherence tomography to measure retinal nerve fiber layer thickness in glaucoma. *Am J Ophthalmol*. 2017;174:1–8.
16. Yoo C, Suh IH, Kim YY. The influence of eccentric scanning of optical coherence tomography on retinal nerve fiber layer analysis in normal subjects. *Ophthalmologica*. 2009;223:326–332.
17. Vizzeri G, Bowd C, Medeiros FA, et al. Effect of improper scan alignment on retinal nerve fiber layer thickness measurements using stratus optical coherence tomograph. *J Glaucoma*. 2008;17:341–349.
18. Hwang YH, Kim MK, Kim DW. Segmentation errors in macular ganglion cell analysis as determined by optical coherence tomography. *Ophthalmology*. 2016;123:950–958.
19. Chen JJ, Kardon RH. Avoiding clinical misinterpretation and artifacts of optical coherence tomography analysis of the optic nerve, retinal nerve fiber layer, and ganglion cell layer. *J Neuro-Ophthalmol*. 2016;36:417–438.
20. Sihota R, Sony P, Gupta V, et al. Diagnostic capability of optical coherence tomography in evaluating the degree of glaucomatous retinal nerve fiber damage. *Invest Ophthalmol Vis Sci*. 2006;47:2006–2010.
21. Pons ME, Ishikawa H, Gürses-Ozden R, et al. Assessment of retinal nerve fiber layer internal reflectivity in eyes with and without glaucoma using optical coherence tomography. *Arch Ophthalmol*. 2000;118:1044–1047.
22. Van Der Schoot J, Vermeer KA, de Boer JF, et al. The effect of glaucoma on the optical attenuation coefficient of the retinal nerve fiber layer in spectral domain optical coherence tomography images.

- Invest Ophthalmol Vis Sci.* 2012;53:2424–2430.
23. Ye C, Yu M, Leung CKS. Impact of segmentation errors and retinal blood vessels on retinal nerve fibre layer measurements using spectral-domain optical coherence tomography. *Acta Ophthalmol.* 2015;94:1–9.
 24. Jonas JB, Nguyen XN, Gusek GC, et al. Parapapillary chorioretinal atrophy in normal and glaucoma eyes. I. Morphometric data. *Invest Ophthalmol Vis Sci.* 1989;30:908–918.
 25. Jonas JB. Clinical implications of peripapillary atrophy in glaucoma. *Curr Opin Ophthalmol.* 2005;16:84–88.